

# A joint explanation of $W$ -mass and muon $g - 2$ in 2HDM

Xiao-Fang Han<sup>1</sup>, Fei Wang<sup>2</sup>, Lei Wang<sup>1</sup>, Jin Min Yang<sup>3,4</sup>, Yang Zhang<sup>2</sup>

<sup>1</sup> *Department of Physics, Yantai University, Yantai 264005, P. R. China*

<sup>2</sup> *School of Physics and Microelectronics,*

*Zhengzhou University, Zhengzhou 450001, P. R. China*

<sup>3</sup> *CAS Key Laboratory of Theoretical Physics, Institute of Theoretical Physics, Chinese Academy of Sciences, Beijing 100190, P. R. China*

<sup>4</sup> *School of Physical Sciences, University of Chinese Academy of Sciences, Beijing 100049, P. R. China*

## Abstract

Since both  $W$ -mass and muon  $g - 2$  can be affected by the mass splittings among extra Higgs bosons ( $H$ ,  $A$ ,  $H^\pm$ ) in a 2HDM, we take a model with  $\mu$ - $\tau$  LFV interactions to examine the two anomalies reported respectively by CDF II and FNAL. We obtain the following observations: (i) Combined with theoretical constraints, the CDF  $W$ -mass measurement disfavors  $H$  or  $A$  to degenerate in mass with  $H^\pm$ , but allows  $H$  and  $A$  to degenerate. The mass splitting between  $H^\pm$  and  $H/A$  is required to be larger than 10 GeV. The  $m_{H^\pm}$  and  $m_A$  are favored to be smaller than 650 GeV for  $m_H < 120$  GeV, and allowed to have more large values with increasing of  $m_H$ . (ii) After imposing other relevant experimental constraints, there are parameter spaces that simultaneously satisfy (at  $2\sigma$  level) the CDF  $W$ -mass, the FNAL muon  $g - 2$  and the data of lepton universality in  $\tau$  decays, but the mass splittings among extra Higgs bosons are strictly constrained.

## I. INTRODUCTION

The CDF collaboration presented their new result for the  $W$ -boson mass measurement [1]

$$m_W = 80.4335 \pm 0.0094 \text{ GeV}. \quad (1)$$

The experimental central value has an approximate  $7\sigma$  discrepancy from the Standard Model (SM) prediction,  $80.357 \pm 0.006$  GeV [2]. On the other hand, there has been a long-standing discrepancy between the SM prediction and experiment for the muon anomalous magnetic moment (muon  $g - 2$ ). The combined result of the FNAL experiment [3] and the BNL experiment [4] has an approximate  $4.2\sigma$  deviation from the SM prediction [5–7]

$$\Delta a_\mu = a_\mu^{exp} - a_\mu^{SM} = (25.1 \pm 5.9) \times 10^{-10}. \quad (2)$$

Both the two deviations strongly imply existence of new physics beyond SM. Some plausible explanations have already performed for the CDF  $W$ -mass [8–41].

Among various new physics models, two-Higgs-doublet models (2HDMs) are rather simple extensions of the SM (for a recent review, see, e.g., [42]). The 2HDM introduces a second  $SU(2)_L$  Higgs doublet and thus predicts two neutral CP-even Higgs bosons  $h$  and  $H$ , one neutral pseudoscalar  $A$  and a pair of charged Higgs boson  $H^\pm$  [43]. The 2HDM can give additional corrections to the masses of gauge bosons via the self-energy diagrams exchanging extra Higgs fields. In addition, if the extra Higgs bosons have appropriate couplings to the leptons, the muon  $g - 2$  can be simply explained. Since both the  $W$ -mass and muon  $g - 2$  can be affected by the mass splittings among  $H$ ,  $A$ , and  $H^\pm$ , in this note we take a 2HDM with the  $\mu$ - $\tau$  lepton flavor violation (LFV) interactions to study the possibility of a simultaneous explanation of both anomalies. In our analysis we will intensively examine the parameter space of this model by considering various relevant theoretical and experimental constraints. For the single explanation of muon  $g - 2$  using the Higgs doublet field with the  $\mu$ - $\tau$  LFV interactions, see e.g., [44–62].

The paper is organized as follows. In Sec. II we will introduce the 2HDM with the  $\mu$ - $\tau$  LFV interactions. In Sec. III and Sec. IV we study the  $W$ -boson mass and muon  $g - 2$  after imposing relevant theoretical and experimental constraints. Finally, we give our conclusion in Sec. V.

TABLE I: Assignment of  $Z_4$  charge in the 2HDM with  $\mu$ - $\tau$ -philic Higgs doublet.

	$\phi_1$	$\phi_2$	$Q_L^i$	$U_R^i$	$D_R^i$	$L_L^e$	$L_L^\mu$	$L_L^\tau$	$e_R$	$\mu_R$	$\tau_R$
$Z_4$	1	-1	1	1	1	1	$i$	$-i$	1	$i$	$-i$

## II. A TWO-HIGGS-DOUBLET MODEL WITH $\mu$ - $\tau$ LFV INTERACTIONS

The 2HDM with the  $\mu$ - $\tau$  LFV interactions may be derived from a general 2HDM by take specific parameters. Also it can be naturally obtained by introducing an inert Higgs doublet  $\phi_2$  under a discrete  $Z_4$  symmetry, and the  $Z_4$  charge assignment is displaced in Table I [53]. The Higgs potential with the  $Z_4$  symmetry is given by

$$\begin{aligned}
 V = & Y_1(\phi_1^\dagger\phi_1) + Y_2(\phi_2^\dagger\phi_2) + \frac{\lambda_1}{2}(\phi_1^\dagger\phi_1)^2 + \frac{\lambda_2}{2}(\phi_2^\dagger\phi_2)^2 \\
 & + \lambda_3(\phi_1^\dagger\phi_1)(\phi_2^\dagger\phi_2) + \lambda_4(\phi_1^\dagger\phi_2)(\phi_2^\dagger\phi_1) + \left[ \frac{\lambda_5}{2}(\phi_1^\dagger\phi_2)^2 + \text{h.c.} \right]. \quad (3)
 \end{aligned}$$

Here all the parameters are real. Although  $\lambda_5$  is the only possible complex parameter, it can be rendered real with a phase redefinition of one of the two Higgs fields. The two Higgs doublets  $\phi_1$  and  $\phi_2$  are expressed by

$$\phi_1 = \begin{pmatrix} G^+ \\ \frac{1}{\sqrt{2}}(v + h + iG^0) \end{pmatrix}, \quad \phi_2 = \begin{pmatrix} H^+ \\ \frac{1}{\sqrt{2}}(H + iA) \end{pmatrix}.$$

The  $\phi_1$  field obtains a nonzero vacuum expectation value (VEV),  $v=246$  GeV, while the  $\phi_2$  field has zero VEV. The parameter  $Y_1$  can be determined from the minimization condition for the Higgs potential,

$$Y_1 = -\frac{1}{2}\lambda_1 v^2. \quad (4)$$

The fields  $G^0$  and  $G^+$  indicate Nambu-Goldstone bosons, which are eaten by the gauge bosons. The fields  $A$  and  $H^+$  represent the mass eigenstates of the CP-odd Higgs boson and charged Higgs boson, whose masses are written as

$$m_{H^\pm}^2 = Y_2 + \frac{\lambda_3}{2}v^2, \quad m_A^2 = m_{H^\pm}^2 + \frac{1}{2}(\lambda_4 - \lambda_5)v^2. \quad (5)$$

There is no mixing between the two CP-even Higgs bosons  $h$  and  $H$ , and their masses are

$$m_h^2 = \lambda_1 v^2 \equiv (125 \text{ GeV})^2, \quad m_H^2 = m_A^2 + \lambda_5 v^2. \quad (6)$$

We obtain the masses of fermions via the Yukawa interactions with  $\phi_1$ ,

$$-\mathcal{L} = y_u \bar{Q}_L \tilde{\phi}_1 U_R + y_d \bar{Q}_L \phi_1 D_R + y_\ell \bar{L}_L \phi_1 E_R + \text{h.c.}, \quad (7)$$

where  $\tilde{\phi}_1 = i\tau_2\phi_1^*$ , and  $E_R$ ,  $U_R$  and  $D_R$  stand for the three generations of right-handed fermion fields for the charged leptons, up-type quarks and down-type quarks. We define  $L_L = (v_{L_i}, \ell_{L_i})^T$  and  $Q_L = (u_{L_i}, d_{L_i})^T$  with  $i$  representing generation indices. Under the  $Z_4$  symmetry, the lepton Yukawa matrix  $y_\ell$  is diagonal and therefore the lepton fields ( $L_L$ ,  $E_R$ ) are mass eigenstates.

Under the  $Z_4$  symmetry, the  $\phi_2$  doublet is allowed to have  $\mu$ - $\tau$  interactions [53],

$$-\mathcal{L}_{LFV} = \sqrt{2} \rho_{\mu\tau} \overline{L}_L^\mu \phi_2 \tau_R + \sqrt{2} \rho_{\tau\mu} \overline{L}_L^\tau \phi_2 \mu_R + \text{h.c.} . \quad (8)$$

The additional Higgs bosons  $H$ ,  $A$  and  $H^\pm$  only have  $\mu$ - $\tau$  LFV Yukawa couplings. On the other hand, the SM-like Higgs boson  $h$  has exactly same couplings to the gauge bosons and fermions as the SM Higgs, with no  $\mu$ - $\tau$  LFV couplings at the tree level.

### III. THE $S$ , $T$ , $U$ PARAMETERS AND $W$ -MASS

The model can produce main corrections to the masses of gauge bosons via self-energy diagrams exchanging extra Higgs fields. The oblique parameters ( $S$ ,  $T$ ,  $U$ ) [63, 64] represent radiative corrections to the two-point functions of gauge bosons. Most effects on precision measurements can be described by these parameters. Recently, Ref. [9] gave the values of these parameters from an analysis of precision electroweak data including the CDF new result of the  $W$ -mass,

$$S = 0.06 \pm 0.10, \quad T = 0.11 \pm 0.12, \quad U = 0.14 \pm 0.09. \quad (9)$$

The correlation coefficients are given by

$$\rho_{ST} = 0.9, \quad \rho_{SU} = -0.59, \quad \rho_{TU} = -0.85. \quad (10)$$

The  $W$ -boson mass can be inferred from the following relation [64],

$$\Delta m_W^2 = \frac{\alpha c_W^2}{c_W^2 - s_W^2} m_Z^2 \left( -\frac{1}{2} S + c_W^2 T + \frac{c_W^2 - s_W^2}{4s_W^2} U \right). \quad (11)$$

In our analysis, we adopt 2HDMC [65] to calculate the 2HDM corrections to  $S$ ,  $T$ ,  $U$  parameters, and perform a global fit to the predictions of  $S$ ,  $T$ ,  $U$  parameters. As the global fit results are presented on two-dimension planes, a limit of  $\chi^2 < \chi_{\min}^2 + 6.18$  is set to obtain  $2\sigma$  favored regions, where  $\chi_{\min}^2$  is the minimum of  $\chi^2$  corresponding the best fit

point. In addition, we consider theoretical constraints from perturbativity, vacuum stability and unitarity, which are described in detail in Appendix A.

We scan  $m_H$ ,  $m_A$  and  $m_{H^\pm}$  parameters in the following ranges:

$$\begin{aligned} 80 \text{ GeV} < m_{H^\pm} < 1000 \text{ GeV}, \quad 65 \text{ GeV} < m_A < 1000 \text{ GeV}, \\ 10 \text{ GeV} < m_H < 120 \text{ GeV}, \quad 130 \text{ GeV} < m_H < 1000 \text{ GeV}. \end{aligned} \quad (12)$$

In Fig. 1 and Fig. 2, we show the samples explaining the CDF  $W$ -boson mass measurement within  $2\sigma$  range while satisfying the constraints of the oblique parameters and theory. From Fig. 1 and Fig. 2, we see that  $H$  or  $A$  is disfavored to exactly degenerate in mass with  $H^\pm$ , but their masses are allowed to be degenerate. The mass splitting between  $H^\pm$  and  $H/A$  is imposed upper and lower bounds, and required to be approximately larger than 10 GeV. When one of  $m_H$  and  $m_A$  is close to  $m_{H^\pm}$ , the other is allowed to have sizable deviation from  $m_{H^\pm}$ . The  $m_{H^\pm}$  and  $m_A$  are favored to be smaller than 650 GeV for  $m_H < 120$  GeV (see Fig. 2), and allowed to have more large values with increasing of  $m_H$  (see Fig. 1).

Now we analyze the reason. In the model, the correction to the  $T$  parameter is expressed as

$$T = \frac{1}{16\pi M_W^2 s_W^2} \left\{ \left[ \mathcal{F}(M_{H^\pm}^2, M_H^2) - \mathcal{F}(M_H^2, M_A^2) + \mathcal{F}(M_{H^\pm}^2, M_A^2) \right] \right\}, \quad (13)$$

where the  $\mathcal{F}$  function is [66–68]

$$\mathcal{F}(m_1^2, m_2^2) = \frac{1}{2} (m_1^2 + m_2^2) - \frac{m_1^2 m_2^2}{m_1^2 - m_2^2} \log \left( \frac{m_1^2}{m_2^2} \right). \quad (14)$$

The function  $\frac{\mathcal{F}(m_1^2, m_2^2)}{m_W^2}$  and the factor  $\frac{1}{16\pi s_W^2}$  in the  $T$  parameter are usually larger than those of  $S$  and  $U$  parameters. Therefore, in general one expects  $T$  to be dominant in the oblique corrections. There are detailed discussions in Ref. [69]. The expressions in Eq. (13) and Eq. (14) show that the  $T$  parameter is sensitive to the mass splittings among  $H$ ,  $A$  and  $H^\pm$ . The  $T$  parameter will be zero for  $m_H = m_{H^\pm}$  or  $m_A = m_{H^\pm}$ , but takes a non-zero value for  $m_A = m_H$ . Therefore, the corrections of the model to the oblique parameters tend to become small as one of  $m_H$  and  $m_A$  approaches to  $m_{H^\pm}$ . However, in order to accommodate the  $W$ -mass reported by the CDF II collaboration, the model needs to produce an appropriate value of  $T$ , which excludes  $m_H = m_{H^\pm}$  or  $m_A = m_{H^\pm}$ .

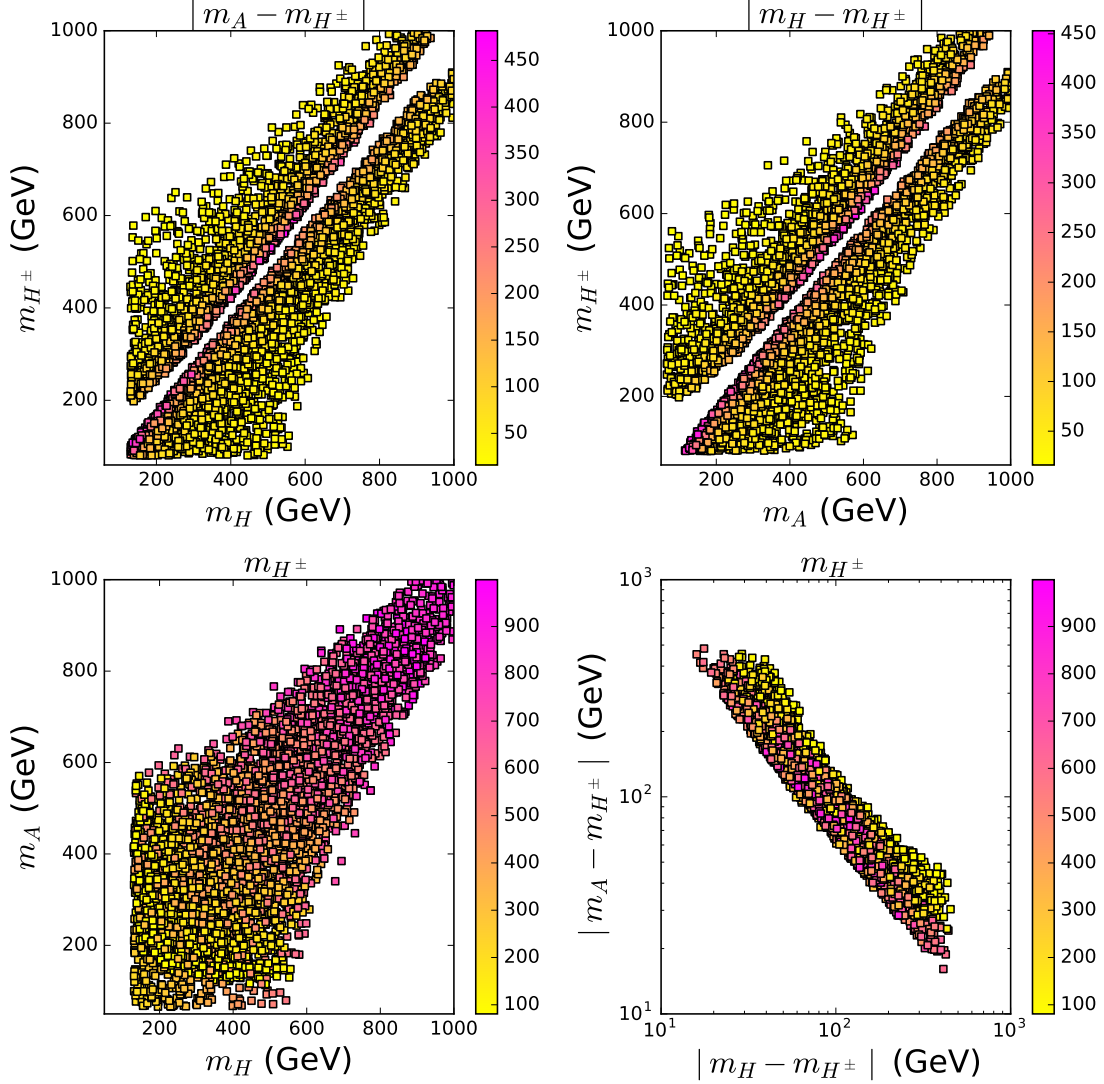


FIG. 1: For  $m_H > 130$  GeV, the samples explaining the CDF II results of the  $W$ -mass within  $2\sigma$  range while satisfying the constraints of the oblique parameters and theoretical constraints. The varying colors in each panel indicate the values of  $|m_A - m_{H^\pm}|$ ,  $|m_H - m_{H^\pm}|$  and  $m_{H^\pm}$ , respectively.

#### IV. MUON $g - 2$ , $\tau$ DECAYS, AND OTHER RELEVANT CONSTRAINTS

The model gives additional corrections to the muon  $g - 2$  anomaly ( $\Delta a_\mu$ ) via the one-loop diagrams involving the  $\mu - \tau$  LFV couplings of  $H$  and  $A$  [44–46],

$$\Delta a_\mu = \frac{m_\mu m_\tau \rho^2}{8\pi^2} \left[ \frac{(\log \frac{m_H^2}{m_\tau^2} - \frac{3}{2})}{m_H^2} - \frac{\log(\frac{m_A^2}{m_\tau^2} - \frac{3}{2})}{m_A^2} \right]. \quad (15)$$

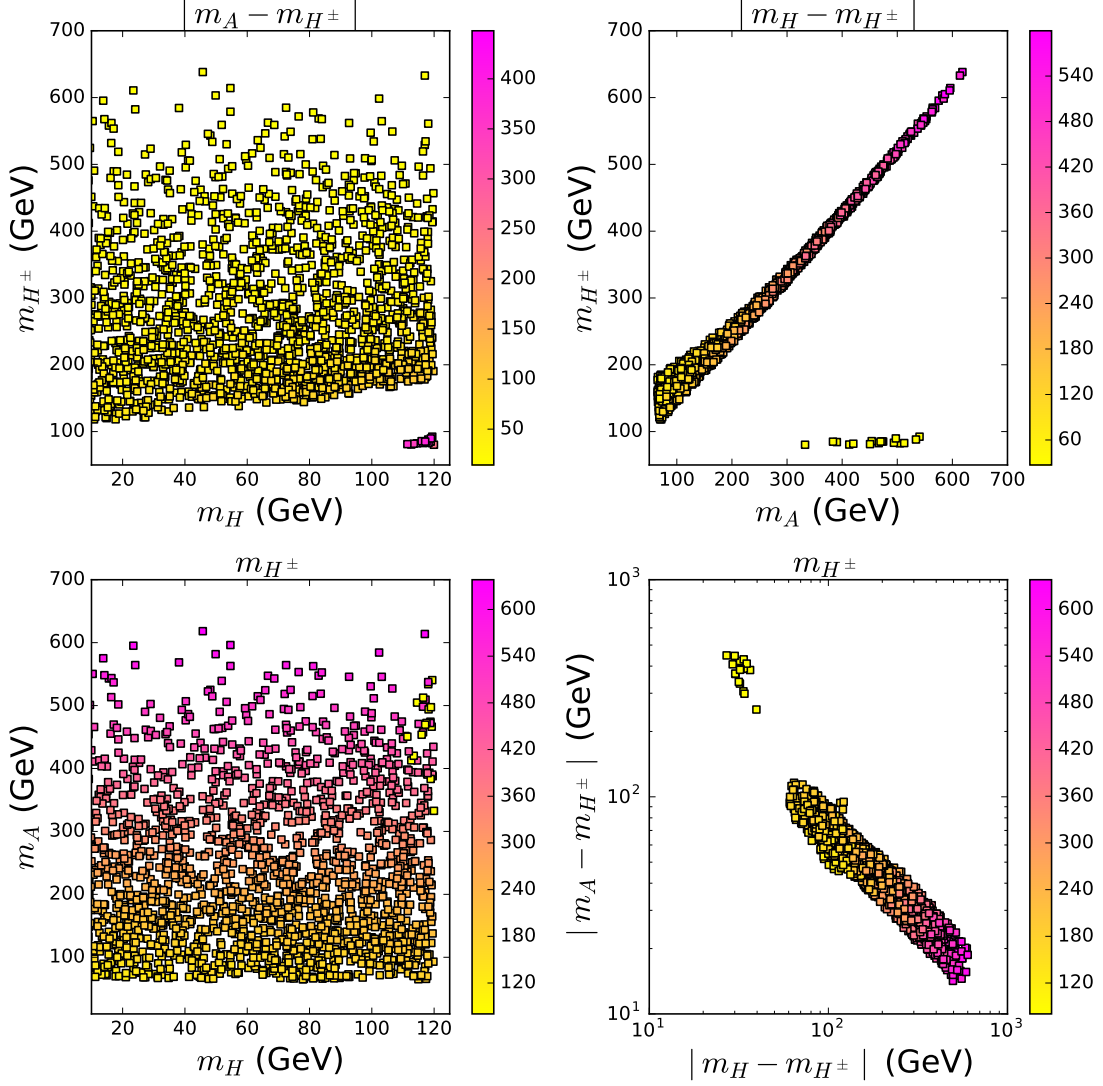


FIG. 2: Same as Fig. 1, but for  $m_H < 120$  GeV.

Here we find  $\Delta a_\mu > 0$  for  $m_A > m_H$ .

Because the extra Higgs bosons have the  $\mu$ - $\tau$  LFV interactions, the model can affect the lepton flavor universality (LFU) in the  $\tau$  lepton decays. The HFAG collaboration tests the LFU from ratios of the partial widths of a heavier lepton. They obtains [70]

$$\left(\frac{g_\tau}{g_\mu}\right) = 1.0011 \pm 0.0015, \quad \left(\frac{g_\tau}{g_e}\right) = 1.0029 \pm 0.0015, \quad \left(\frac{g_\mu}{g_e}\right) = 1.0018 \pm 0.0014, \quad (16)$$

using pure leptonic processes, namely

$$\left(\frac{g_\tau}{g_\mu}\right)^2 \equiv \frac{\bar{\Gamma}(\tau \rightarrow e\nu\bar{\nu})}{\bar{\Gamma}(\mu \rightarrow e\nu\bar{\nu})}, \quad (17)$$

$$\left(\frac{g_\tau}{g_e}\right)^2 \equiv \frac{\bar{\Gamma}(\tau \rightarrow \mu\nu\bar{\nu})}{\bar{\Gamma}(\mu \rightarrow e\nu\bar{\nu})}, \quad (18)$$

$$\left(\frac{g_\mu}{g_e}\right)^2 \equiv \frac{\bar{\Gamma}(\tau \rightarrow \mu\nu\bar{\nu})}{\bar{\Gamma}(\tau \rightarrow e\nu\bar{\nu})}, \quad (19)$$

with  $\bar{\Gamma}$  representing the partial width which is normalized by the corresponding SM value.  $g_e$  ( $g_{\mu,\tau}$ ) denote the effective couplings between  $e$  ( $\mu, \tau$ ) and  $\nu_e$  ( $\nu_\mu, \nu_\tau$ ). With the two semi-hadronic processes,

$$\left(\frac{g_\tau}{g_\mu}\right)_h^2 \equiv \frac{\text{Br}(\tau \rightarrow h\nu)}{\text{Br}(h \rightarrow \mu\bar{\nu})} \frac{2m_h m_\mu^2 \tau_h}{(1 + \delta_h) m_\tau^2 \tau_\tau} \left(\frac{1 - m_\mu^2/m_h^2}{1 - m_h^2/m_\tau^2}\right)^2, \quad (20)$$

where  $h$  indicates  $\pi$  or  $K$ , they measure

$$\left(\frac{g_\tau}{g_\mu}\right)_\pi = 0.9963 \pm 0.0027, \quad \left(\frac{g_\tau}{g_\mu}\right)_K = 0.9858 \pm 0.0071. \quad (21)$$

The statistical correlation matrix for the five fitted coupling ratios is

$$\begin{bmatrix} 1 & 53\% & -49\% & 24\% & 12\% \\ 53\% & 1 & 48\% & 26\% & 10\% \\ -49\% & 48\% & 1 & 2\% & -2\% \\ 24\% & 26\% & 2\% & 1 & 5\% \\ 12\% & 10\% & -2\% & 5\% & 1 \end{bmatrix}. \quad (22)$$

In this model, we can calculate

$$\begin{aligned} \bar{\Gamma}(\tau \rightarrow \mu\nu\bar{\nu}) &= (1 + \delta_{\text{loop}}^\tau)^2 (1 + \delta_{\text{loop}}^\mu)^2 + \delta_{\text{tree}}, \\ \bar{\Gamma}(\tau \rightarrow e\nu\bar{\nu}) &= (1 + \delta_{\text{loop}}^\tau)^2, \\ \bar{\Gamma}(\mu \rightarrow e\nu\bar{\nu}) &= (1 + \delta_{\text{loop}}^\mu)^2. \end{aligned} \quad (23)$$

The tree-level correction  $\delta_{\text{tree}}$  is from the contribution of  $H^\pm$  to  $\tau \rightarrow \mu\nu\bar{\nu}$ ,

$$\delta_{\text{tree}} = 4 \frac{m_W^4 \rho^4}{g^4 m_{H^\pm}^4}, \quad (24)$$

which can give a positive correction.  $\delta_{\text{loop}}^\mu$  and  $\delta_{\text{loop}}^\tau$  are the corrections to vertices  $W\bar{\nu}_\mu\mu$  and  $W\bar{\nu}_\tau\tau$  from the one-loop diagrams containing  $A$ ,  $H$ , and  $H^\pm$ , respectively. As we assume  $\rho_{\mu\tau} = \rho_{\tau\mu}$  in the lepton Yukawa matrix, the two corrections are identical [53, 71, 72],

$$\delta_{\text{loop}}^\tau = \delta_{\text{loop}}^\mu = \frac{1}{16\pi^2} \rho^2 \left[ 1 + \frac{1}{4} (H(x_A) + H(x_H)) \right], \quad (25)$$



where  $H(x_\phi) \equiv \ln(x_\phi)(1+x_\phi)/(1-x_\phi)$  with  $x_\phi = m_\phi^2/m_{H^\pm}^2$ . Meanwhile, for the semi-hadronic processes, we have

$$\left(\frac{g_\tau}{g_\mu}\right) = \left(\frac{g_\tau}{g_\mu}\right)_K = \left(\frac{g_\tau}{g_\mu}\right)_\pi. \quad (26)$$

In our study, we perform a global fit to the predictions of these five ratios. Note that there is a vanishing eigenvalue in the covariance matrix constructed from Eq. (16), Eq. (21) and Eq. (22), and therefore such a degree of freedom is removed. With remaining four degrees of freedom, the  $2\sigma$  confidence level region is obtained by adopting a limit of  $\chi_\tau^2 < 9.72$ . Thus, the surviving samples are much more consistent with the experimental results than the SM, which has a  $\chi_\tau^2$  of 12.25. Also the model can affect the LFU in the  $Z$ -boson decays [73], and the constraints from the  $Z$ -boson decays are generally weaker than those from the  $\tau$  decays.

In the model, the fields  $H$ ,  $A$  and  $H^\pm$  have no couplings to quarks, and therefore they are produced at the LHC mainly via the electroweak processes,  $pp \rightarrow W^{\pm*} \rightarrow H^\pm A/H$ ,  $pp \rightarrow Z^* \rightarrow HA$  and  $pp \rightarrow Z^*/\gamma^* \rightarrow H^+H^-$ . The final state signal mainly includes multi-leptons, and therefore the multi-lepton event searches at the LHC can impose stringent constraints which require  $m_H$  to be larger than 560 GeV [55]. Also a very light  $H$  may escape the constraints of the direct searches at the LHC [56]. In this case, the explanation of muon  $g-2$  anomaly requires a very small  $\rho$ , which leads that the contributions of the model to the  $\tau$  decays are too small to explain the data of LFU in the  $\tau$  decays. Therefore, in this work we discuss the scenario of  $m_H > 560$  GeV. In addition, to respect the perturbativity we choose the Yukawa coupling parameter  $\rho < 1$ .

At the tree level, the 125 GeV Higgs has the same couplings to the SM particles as in the SM. The  $h \rightarrow \gamma\gamma$  decay will be corrected by the one-loop diagram of the charged Higgs [74]. We consider the bound of the diphoton signal strength [2],

$$\mu_{\gamma\gamma} = 1.11_{-0.09}^{+0.1}. \quad (27)$$

In Fig. 3, we project the surviving samples explaining the muon  $g-2$  anomaly and the LFU in  $\tau$ -decays within  $2\sigma$  ranges, with other relevant constraints from the theory, the oblique parameters, the CDF II  $W$ -mass and the diphoton signal data of the 125 GeV Higgs being satisfied. Eq. (15) shows that  $H$  and  $A$  respectively give positive and negative contributions to the muon  $g-2$ , and their contributions are suppressed by their masses. Therefore, the explanation of muon  $g-2$  requires  $m_A > m_H$  and  $\rho$  to become large with increasing of  $m_H$  and decreasing of  $(m_A - m_H)$  (see the upper-left panel).

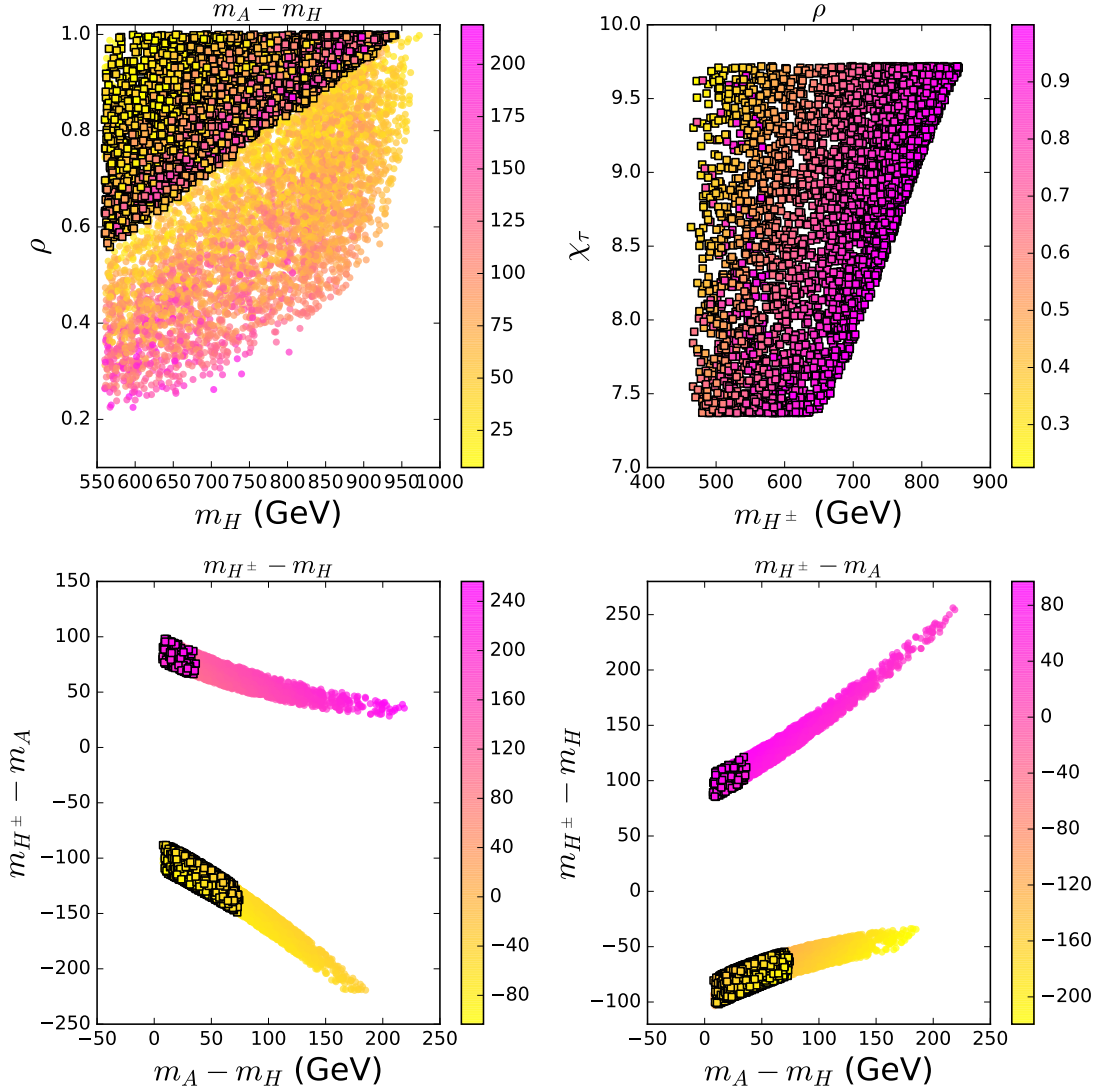


FIG. 3: The bullets can explain the muon  $g - 2$  within  $2\sigma$  range, while the squares can explain the muon  $g - 2$  and the  $\tau$ -decays within  $2\sigma$  ranges while satisfying the constraints of  $Z$ -decays. Other relevant constraints from the theory, the oblique parameters, the CDF II  $W$ -mass and the diphoton signal data of the 125 GeV Higgs are also satisfied. The varying colors in each panel indicate the values of  $m_A - m_H$ ,  $\rho$ ,  $m_{H^\pm} - m_H$  and  $m_{H^\pm} - m_A$ , respectively.

The ratio  $\left(\frac{g_\tau}{g_e}\right)$  in the  $\tau$  decays has approximately  $2\sigma$  deviation from the SM. Therefore, enhancing  $\Gamma(\tau \rightarrow \mu\nu\bar{\nu})$  may give a better fit to the data of LFU in the  $\tau$  decays. The decay  $\tau \rightarrow \mu\nu\nu$  obtains a positive correction from the  $\delta_{\text{tree}}$  term of Eq. (23). Such a term is from the tree-level diagram mediated by the charged Higgs, and proportional to  $\rho^4/m_{H^\pm}^2$ . Therefore, the upper-right panel of Fig. 3 shows that the value of  $\chi_\tau^2$  tends to become

large with increasing of  $m_{H^\pm}$  and decreasing of  $\rho$ . In addition, because of the constraints of the oblique parameters and  $W$ -boson mass, the upper-left panel of Fig. 1 shows that  $m_{H^\pm}$  tends to increase with  $m_H$ , especially for a large  $m_H$ , which implies that the value of  $\chi_\tau^2$  becomes large with increasing of  $m_H$ . Therefore, the upper-left panel of Fig. 3 shows that a simultaneous explanation of the muon  $g - 2$  and LFU in  $\tau$  decays favors a large  $\rho$  which increases with  $m_H$ .

From the lower panel of Fig. 3, we see that the mass splittings among  $H$ ,  $A$  and  $H^\pm$  are stringently constrained in the region simultaneously explaining the  $W$ -mass, muon  $g - 2$  and LFU in  $\tau$  decays, i.e.,  $10 \text{ GeV} < m_A - m_H < 75 \text{ GeV}$ ,  $65 \text{ GeV} < m_{H^\pm} - m_A < 100 \text{ GeV}$ ,  $85 \text{ GeV} < m_{H^\pm} - m_H < 125 \text{ GeV}$  ( $-150 \text{ GeV} < m_{H^\pm} - m_A < -85 \text{ GeV}$ ,  $-105 \text{ GeV} < m_{H^\pm} - m_H < -55 \text{ GeV}$ ).

In the model, pair productions of extra Higgs bosons via electroweak processes at LHC lead to detectable multi-leptons signal containing  $\mu$  and  $\tau$ . The current lower bound of 560 GeV on  $m_H$  is mainly obtained from the CMS search for electroweak production of charginos and neutralinos in multilepton final states [75]. By naively normalizing number of background and signal events, the lower bound on  $m_H$  can be pushed to 700 GeV for 300  $\text{fb}^{-1}$  integrated luminosity data. Adopting the same procedure, we estimate that it needs more than 3000  $\text{fb}^{-1}$  integrated luminosity data to cover the whole surviving parameter, namely  $m_H < 950 \text{ GeV}$ . However, this CMS search is originally designed for searching SUSY particles. A dedicated study, focusing on  $\mu\tau$  final states and improving signal regions for high mass region, can greatly reduce the required integrated luminosity to acceptable level, which is beyond the scope of this paper.

## V. CONCLUSION

We examine the CDF II  $W$ -boson mass and the FNAL muon  $g - 2$  in the 2HDM in which the extra Higgs doublet has the  $\mu$ - $\tau$  LFV interactions. Imposing the theoretical constraints, we found that the CDF II  $W$ -boson mass disfavors  $H$  or  $A$  to degenerate in mass with  $H^\pm$ , and the mass splitting between  $H^\pm$  and  $H/A$  is favored to be larger than 10 GeV. The  $m_{H^\pm}$  and  $m_A$  are favored to be smaller than 650 GeV for  $m_H < 120 \text{ GeV}$ , and allowed to have more large values with increasing of  $m_H$ . Considering other relevant experimental constraints, we found that the mass splittings among  $H$ ,  $A$  and  $H^\pm$  are stringently restricted

in the parameter space which can simultaneously explain the CDF II  $W$ -mass, the FNAL muon  $g - 2$ , and the data of LFU in the  $\tau$  decays.

## Acknowledgment

We thank Lei Wu for helpful discussions. This work was supported by the National Natural Science Foundation of China under grants 11975013, 12105248, 11821505, 12075300, 12075213, by Peng-Huan-Wu Theoretical Physics Innovation Center (12047503), by the CAS Center for Excellence in Particle Physics (CCEPP), and by the Key Research Program of the Chinese Academy of Sciences, Grant NO. XDPB15.

## Appendix A: Theoretical constraints

### 1. Perturbativity

The quartic couplings of the scalar potential in Eq. (3) cannot be too large individually, for otherwise the theory will no longer be perturbative. Thus we demand

$$|\lambda_{1,2,3,4,5}| \leq 4\pi. \quad (\text{A1})$$

### 2. Vacuum stability

Vacuum stability requires the potential to be bounded from below and stay positive for arbitrarily large values of the fields. The requirement leads to restrictions on the parameters of the model,

$$\lambda_1 > 0, \quad \lambda_2 > 0, \quad \lambda_3 + \sqrt{\lambda_1 \lambda_2} > 0, \quad \lambda_3 + \lambda_4 - |\lambda_5| + \sqrt{\lambda_1 \lambda_2} > 0. \quad (\text{A2})$$

### 3. Unitarity

The amplitudes for scalar-scalar scattering  $s_1 s_2 \rightarrow s_3 s_4$  at high energies respect unitarity, which leads to the following bounds on the parameters of the model [76, 77],

$$|a_{\pm}|, |b_{\pm}|, |c_{\pm}|, |e_{\pm}|, |f_{\pm}|, |g_{\pm}| \leq 8\pi, \quad (\text{A3})$$

with

$$a_{\pm} = \frac{3}{2}(\lambda_1 + \lambda_2) \pm \sqrt{\frac{9}{4}(\lambda_1 - \lambda_2)^2 + (2\lambda_3 + \lambda_4)^2}, \quad (\text{A4})$$

$$b_{\pm} = \frac{1}{2}(\lambda_1 + \lambda_2) \pm \sqrt{\frac{1}{4}(\lambda_1 - \lambda_2)^2 + \lambda_4^2}, \quad (\text{A5})$$

$$c_{\pm} = \frac{1}{2}(\lambda_1 + \lambda_2) \pm \sqrt{\frac{1}{4}(\lambda_1 - \lambda_2)^2 + \lambda_5^2}, \quad (\text{A6})$$

$$\mathbf{e}_{\pm} = \lambda_3 + 2\lambda_4 \pm 3\lambda_5, \quad (\text{A7})$$

$$\mathbf{f}_{\pm} = \lambda_3 \pm \lambda_4, \quad (\text{A8})$$

$$\mathbf{g}_{\pm} = \lambda_3 \pm \lambda_5. \quad (\text{A9})$$

- [1] CDF Collaboration, *Science* **376**, 6589 (2022).
- [2] P. A. Zyla et al. [Particle Data Group], “Review of Particle Physics,” *PTEP* **2020**, (2020) 083C01.
- [3] B. Abi *et al.* [Fermilab Collaboration], *Phys. Rev. Lett.* **126**, (2021) 141801.
- [4] Muon  $g-2$  Collaboration, *Phys. Rev. Lett.* **86**, (2001) 2227; *Phys. Rev. D* **73**, (2006) 072003.
- [5] T. Aoyama, N. Asmussen, M. Benayoun, J. Bijnens, T. Blum, *Phys. Rept.* **887**, (2020) 1-166.
- [6] T. Blum, N. Christ, M. Hayakawa, T. Izubuchi, L. Jin, C. Jung, and C. Lehner, *Phys. Rev. Lett.* **124**, 132002 (2020).
- [7] G. Colangelo, F. Hagelstein, M. Hoferichter, L. Laub, P. Stoffer, *JHEP* **03**, 101 (2020).
- [8] Y.-Z. Fan, T.-P. Tang, Y.-L. S. Tsai, L. Wu, arXiv:2204.03693.
- [9] C.-T. Lu, L. Wu, Y. Wu, B. Zhu, arXiv:2204.03796.
- [10] P. Athron, A. Fowlie, C.-T. Lu, L. Wu, Y. Wu, B. Zhu, arXiv:2204.03996.
- [11] G.-W. Yuan, L. Zu, L. Feng, Y.-F. Cai, arXiv:2204.04183.
- [12] A. Strumia, arXiv:2204.04191.
- [13] J. M. Yang, Y. Zhang, *Science Bulletin*, doi: 10.1016/j.scib.2022.06.007, arXiv:2204.04202.
- [14] J. d. Blas, M. Pierini, L. Reina, L. Silvestrini, arXiv:2204.04204.
- [15] X. Du, Z. Li, F. Wang, Y. K. Zhang, arXiv:2204.04286.
- [16] T.-P. Tang, M. Abdughani, L. Feng, Y.-L. S. Tsai, Y.-Z. Fan, arXiv:2204.04356.
- [17] G. Cacciapaglia, F. Sannino, arXiv:2204.04514.
- [18] M. Blennow, P. Coloma, E. Fernandez-Martinez, M. Gonzalez-Lopez, arXiv:2204.04559.

- [19] K. Sakurai, F. Takahashi, W. Yin, arXiv:2204.04770.
- [20] J. J. Fan, L. Li, T. Liu, K.-F. Lyu, arXiv:2204.04805.
- [21] X. Liu, S.-Y. Guo, B. Zhu, Y. Li, arXiv:2204.04834.
- [22] H. M. Lee, K. Yamashita, arXiv:2204.05024.
- [23] Y. Cheng, X.-G. He, Z.-L. Huang, M.-W. Li, arXiv:2204.05031.
- [24] H. Song, W. Su, M. Zhang, arXiv:2204.05085.
- [25] E. Bagnaschi, J. Ellis, M. Madigan, K. Mimasu, V. Sanz, T. You, arXiv:2204.05260.
- [26] A. Paul, M. Valli, arXiv:2204.05267.
- [27] H. Bahl, J. Braathen, G. Weiglein, arXiv:2204.05269.
- [28] P. Asadi, C. Cesarotti, K. Fraser, S. Homiller, A. Parikh, arXiv:2204.05283.
- [29] L. D. Luzio, R. Grober, P. Paradisi, arXiv:2204.05284.
- [30] P. Athron, M. Bach, D. H. J. Jacob, W. Kotlarski, D. Stockinger, A. Voigt, arXiv:2204.05285.
- [31] J. Gu, Z. Liu, T. Ma, J. Shu, arXiv:2204.05296.
- [32] J. J. Heckman, arXiv:2204.05302.
- [33] K. S. Babu, S. Jana, P. K. Vishnu, arXiv:2204.05303.
- [34] B.-Y. Zhu, S. Li, J.-G. Cheng, R.-L. Li, Y.-F. Liang, arXiv:2204.04688.
- [35] Y. Heo, D.-W. Jung, J. S. Lee, arXiv:2204.05728.
- [36] X. K. Du, Z. Li, F. Wang, Y. K. Zhang, arXiv:2204.05760.
- [37] K. Cheung, W.-Y. Keung, P.-Y. Tseng, arXiv:2204.05942.
- [38] A. Crivellin, M. Kirk, T. Kitahara, F. Mescia, arXiv:2204.05962.
- [39] M. Endo, S. Mishima, arXiv:2204.05965.
- [40] T. Biekotter, S. Heinemeyer, G. Weiglein, arXiv:2204.05975.
- [41] R. Balkin, E. Madge, T. Menzo, G. Perez, Y. Soreq, J. Zupan, arXiv:2204.05992.
- [42] L. Wang, J. M. Yang, Y. Zhang, arXiv:2203.07244.
- [43] T. D. Lee, Phys. Rev. D **8**, (1973) 1226.
- [44] Y. Zhou, Y.-L. Wu, Eur. Phys. Jour. C **27**, (2003) 577.
- [45] K. Adikle Assamagan, A. Deandrea, P.-A. Delsart, Phys. Rev. D **67**, (2003) 035001.
- [46] S. Davidson, G. J. Grenier, Phys. Rev. D **81**, (2010) 095016.
- [47] Y. Omura, E. Senaha, K. Tobe, JHEP **1505**, (2015) 028.
- [48] R. Benbrik, C.-H. Chen, T. Nomura, Phys. Rev. D **93**, (2016) 095004.
- [49] Y. Omura, E. Senaha, K. Tobe, Phys. Rev. D **94**, (2016) 055019.

- [50] L. Wang, J. M. Yang, M. Zhang, Y. Zhang, Phys. Lett. B **788**, (2019) 519-529.
- [51] M. Lindner, M. Platscher, F. S. Queiroz, Phys. Rept. **731**, (2018) 1-82.
- [52] L. Wang, S. Yang, X.-F. Han, Nucl. Phys. B **919**, (2017) 123-141.
- [53] Y. Abe, T. Toma, K. Tsumura, JHEP **1906**, (2019) 142.
- [54] S. Iguro, Y. Omura, M. Takeuchi, JHEP **1911**, (2019) 130.
- [55] L. Wang, Y. Zhang, Phys. Rev. D **100**, (2019) 095005.
- [56] H.-X. Wang, L. Wang, Y. Zhang, Eur. Phys. Jour. C **81**, (2021) 1007.
- [57] S. Iguro, Y. Omura, M. Takeuchi, JHEP **09**, (2020) 144.
- [58] A. Crivellin, D. Müller, C. Wiegand, JHEP **06**, (2019) 119.
- [59] A. Das, T. Nomura, H. Okada, S. Roy, Phys. Rev. D **96**, (2017) 075001.
- [60] P. S. B. Dev, R. N. Mohapatra, Y. Zhang, Phys. Rev. Lett. **120**, 221804 (2018).
- [61] T. Nomura, P. Sanyal, JHEP **05**, (2021) 232.
- [62] F. J. Botella, F. Cornet-Gomez, M. Nebot, Phys. Rev. D **102**, (2020) 035023.
- [63] M. E. Peskin and T. Takeuchi, Phys. Rev. Lett. **65**, 964 (1990).
- [64] M. E. Peskin and T. Takeuchi, Phys. Rev. D **46**, (1992) 381-409
- [65] D. Eriksson, J. Rathsman, O. Stål, Comput. Phys. Commun. **181**, (2010) 189.
- [66] H.-J. He, N. Polonsky, S. Su, Phys. Rev. D **64**, (2001) 053004.
- [67] H. E. Haber, D. O'Neil, Phys. Rev. D **83**, (2011) 055017.
- [68] A. Celis, V. Ilisie, A. Pich, JHEP **07**, (2013) 053.
- [69] W. Grimus, L. Lavoura, O. M. Ogreid, P. Osland, Nucl. Phys. B **801**, (2008) 81-96.
- [70] Y. Amhis et al. [Heavy Flavor Averaging Group (HFAG) Collaboration], arXiv:1412.7515.
- [71] T. Abe, R. Sato and K. Yagyu, JHEP **1507**, (2015) 064.
- [72] X.-F. Han, T. Li, L. Wang, Y. Zhang, Phys. Rev. D **99**, (2019) 095034.
- [73] S. Schael et al. [ALEPH and DELPHI and L3 and OPAL and SLD and LEP Electroweak Working Group and SLD Electroweak Group and SLD Heavy Flavour Group Collaborations], Phys. Rept. **427**, (2006) 257.
- [74] L. Wang, X.-F. Han, JHEP **1404**, (2014) 128.
- [75] A. M. Sirunyan *et al.* [CMS Collaboration], JHEP **1803**, (2018) 166.
- [76] S. Kanemura, T. Kubota, E. Takasugi, Phys. Lett. B **313**, (1993) 155.
- [77] A. G. Akerod, A. Arhrib, E. M. Naimi, Phys. Lett. B **490**, (2000) 119.